

Optimal Fuzzy MPPT Control based PSO Algorithm for Photovoltaic System

Fatah Yahiaoui*, Ouahib Guenounou*, Lamine Brikh*, Mohand-Akli Kacimi*
and Ahmed Ouaret*

ABSTRACT

In this paper, we use the particle swarm optimization (PSO) algorithm to improve the performance of the stand-alone photovoltaic (PV) system. This system consists of a PV panel, a DC-DC boost converter, a fuzzy logic controller (FLC) based maximum power point tracker (MPPT) algorithm and a resistive load. The PSO algorithm is used to optimize the membership functions of both input and output variables of FLC so the stand-alone PV system to deliver a maximum power. The optimized FLC is compared to standard FLC based MPPT controller under constant and varying atmospheric conditions. Simulation results show that the optimized FLC gives a better performance compared to standard FLC.

Keywords: PV panel, MPPT, control, fuzzy logic controller, Optimization, PSO.

1. INTRODUCTION

Solar energy is directly converted into electricity by photovoltaic (PV) panel. The generated power from PV panel is mainly dependent on atmospheric conditions, i.e. solar irradiance and ambient temperature. In order to extract the maximal power of PV panel, several maximal power point tracking (MPPT) methods [1-4] were proposed for stand-alone and grid-connected PV systems. Among the proposed methods, ripple correlation control, hill-climbing, perturb and observe (P and O) and incremental conductance are the most used techniques [5-8]. Although these techniques are relatively simple to implement, they suffer from oscillation of the operating point around the maximum power point (MPP), leading to significant energy losses especially in large scale photovoltaic systems. Recently fuzzy control (FC) is used as a maximum power point tracker [9-16]. The use of FC in PV systems is more suitable compared with conventional approaches, and it is reported in [17] that the performance of the fuzzy control based MPPT is better than the conventional (P and O) controller in terms of tracking speed and fluctuations around the MPP under rapid variations of solar irradiance and temperature.

In this work, we propose a more efficiency design of FC based MPPT intended to be used in photovoltaic system. The key idea is to use PSO algorithm to optimize the membership functions of both input and output variables of FC so the stand-alone photovoltaic system delivers a maximum power. PSO algorithm is one of the most powerful optimization techniques and it is able to deal with large search spaces and to locate global optimum without a precise description of the problem [18-24]. Some recent control algorithms are discussed in [25-30].

The paper is organized as follows: Section 2 presents the mathematical model of PV panel. Section 3 describes the structure of the PV system including the FLC as MPP tracker. The particle swarm optimization approach is described in Section 4. In Section 5, we present the simulation results. Finally, a general conclusion is given in Section 6.

* Laboratory of Industrial Technology and Information, Faculty of Technology, University of Bejaia, 06000 Bejaia, Algeria

2. MATHEMATICAL MODEL OF PV PANEL

Figure 1 shows the equivalent electrical circuit of a solar cell [31, 32]. This circuit can be depicted through a single diode connected with a photo current source I_{ph} , an equivalent parallel resistance R_p and an equivalent series resistance R_s .

Eq. (1) shows the equivalent circuit of the current flowing in the diode.

$$I = N_p I_{ph} - N_p I_s \left(\exp \left[\frac{q}{\alpha k T} (V / N_s + I R_s / N_p) \right] - 1 \right) - N_p / R_p \left(\frac{V}{N_s} + \frac{I R_s}{N_p} \right) \quad (1)$$

where,

- I : PV array output current;
- V : PV array output voltage;
- I_{ph} : Solar cell photocurrent;
- q : Electron charge, $1.60217733e^{-19}$ C;
- α : Diode ideality factor (usually between 1 and 5);
- k : Boltzmann's constant, $1.380658e^{-23}$ J/K;
- T : Operating temperature of the cell in degrees Kelvin (K).

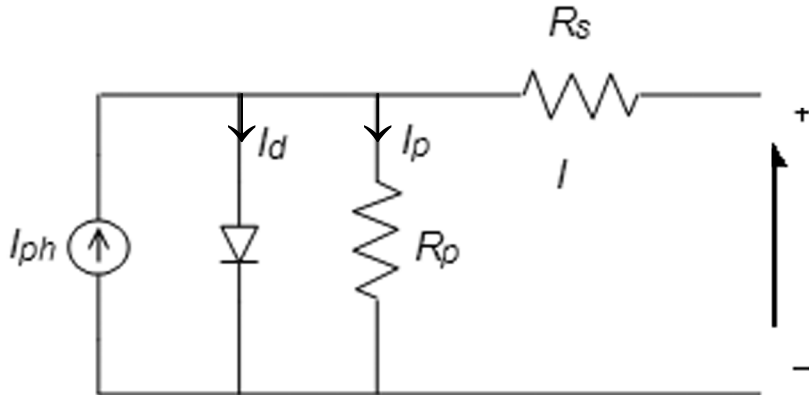


Figure 1: Single diode model of a solar cell

Eq. (2) gives the cell's photocurrent I_{ph} . This last depends on their radiation $S(W/m^2)$ and the temperature $T(K)$:

$$I_{ph} = I_{sc} \left[1 + k_1 \cdot (T - T_r) \right] \frac{S}{1000} \quad (2)$$

where, $k_1 = 0.0017$ A/°C;

- I_{sc} : Cell's short circuit current at the reference temperature;
- T_r : Cell reference temperature (25°C).

The reverse saturation current I_s varies with temperature as stated in the following:

$$I_s = I_{Rs} \left(\frac{T}{T_r} \right)^3 \exp \left[\frac{q}{\alpha k} E_g \left(\frac{1}{T_r} - \frac{1}{T} \right) \right] \quad (3)$$

where,

I_{rs} : Reverse saturation current at T ;

E_g : Bandgap energy of the semiconductor used in the solar cell.

3. PROPOSED PV SYSTEM

As depicted in Figure 2, the developed system contains of a PV panel, a DC–DC boost converter, a controller as an MPP tracker and a resistive load.

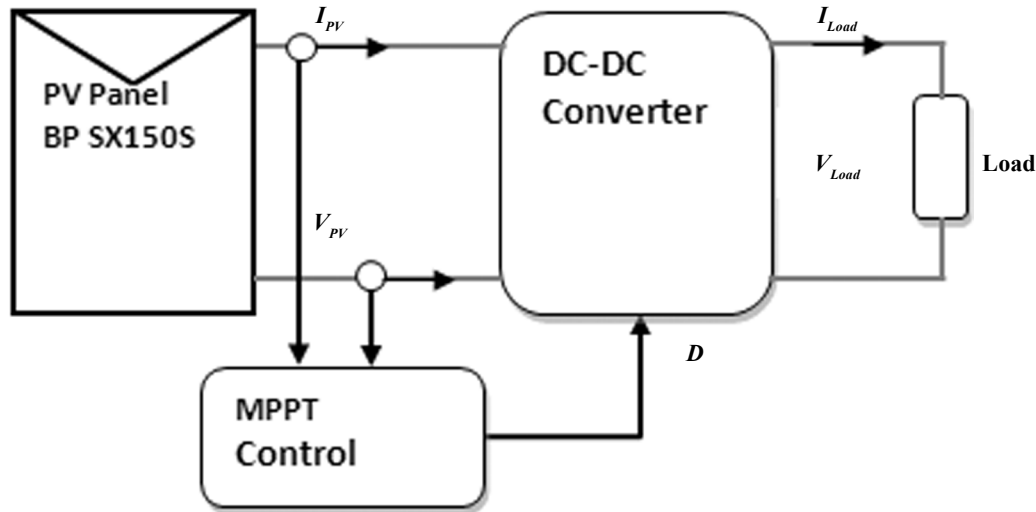


Figure 2: FLC based control MPPT schema of resistive load connected a PV system

3.1. Control of DC-DC Boost Converter

Control of boost converter is used to increase the PV voltage at the input of a resistive charge. The power switch modulates the energy transfer from the input source when the load is controlled by a varying the value of the duty cycle D . In this type of converter, the output voltage is always greater than the input voltage. The relationship of output-input voltage and current can be determined as follows [33-35]:

$$\begin{cases} \frac{V_{Out}}{V_{in}} = \frac{1}{1-D} \\ \frac{I_{in}}{I_{out}} = \frac{1}{1-D} \end{cases} \quad (4)$$

where V_{in} and I_{in} are respectively the voltage and current of input, V_{Out} and I_{out} are respectively the voltage and current of output.

3.2. Fuzzy MPPT controller

3.2.1. Structure of the Fuzzy Controller

The FC contains of three stages in this control algorithm, namely fuzzification, inference engine and defuzzification.

a) Fuzzification Interface

The fuzzification interface makes it to turn a precise greatness or a numerical value $e(k)$ and $\Delta e(k)$ to linguistic values such as Positive Big (PB), Positive Petit (PP) and Negative Petit (NP). The shapes of the membership functions associated with the linguistic variables FLC that we used are linear functions of

triangular type. The partition of fuzzy subsets and the type of membership function, which can adapt shape up to a PV system, are depicted in Figure 3. At a sampling instant k , these two variable inputs are expressed as follows:

$$e(k) = \frac{P(k) - P(k-1)}{V(k) - V(k-1)} \tag{5}$$

$$\Delta e(k) = e(k) - e(k-1) \tag{6}$$

where $P(k)$ is the instantaneous power of the PV array system and $V(k)$ gives the corresponding instantaneous voltage. The $e(k)$ value will show the location of the operating load power point whether on the left or right side of the point of the MPP. The $\Delta e(k)$ indicates the moving direction of the operating power point.

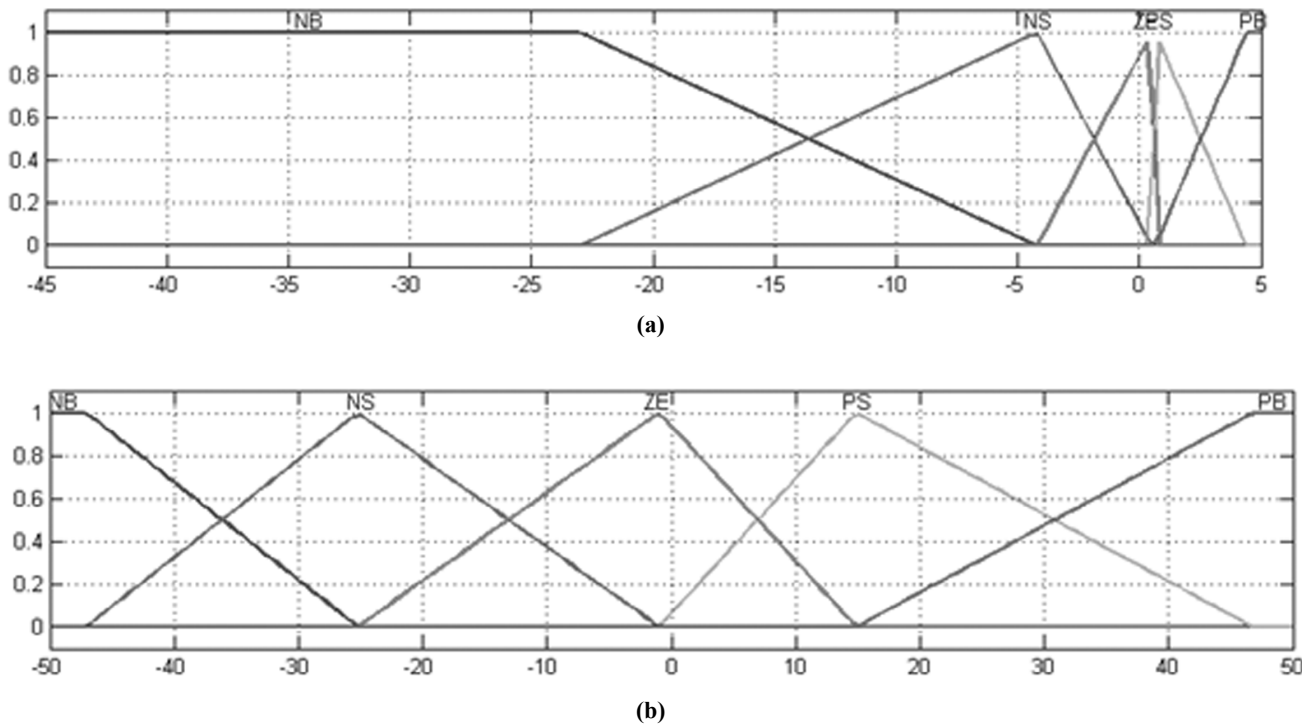


Figure 3: Membership Functions of-(a) and-(b).

b) Inference engine

Table 1 shows the rule table of a fuzzy controller, where two entries and a output of the matrix that are fuzzy sets of error $e(k)$, change of error $\Delta e(k)$ and change of the duty ratio ΔD_N to the converter. The matrix

Table 1
Rule base table for computation ΔD_N .

e	Δe				
	NB	NS	ZE	PS	PB
NB	ZE	ZE	PB	PB	PB
NS	ZE	ZE	PS	PS	PS
ZE	PS	ZE	ZE	ZE	NS
PS	NS	NS	NS	ZE	ZE
PB	NB	NB	NB	ZE	ZE

rows depict the five fuzzy sets of the error, the matrix columns depict the five fuzzy sets of the errors variation and the matrix cells depict the on possible output fuzzy sets giving the normalized incremental change of the duty ratio ΔD_N .

c) Defuzzification interface

Defuzzification for this system is the centre of gravity to compute the output of this FLC which is the duty ration (cycle). The change of duty ratio ΔD_N is determined by the centre of gravity defuzzification method as follows:

$$\Delta D_N(k) = \frac{\sum_{j=1}^n \mu(D_j) - D_j}{\sum_{j=1}^n \mu(D_j)} \quad (7)$$

The output of fuzzy logic controller is the change of duty ratio ΔD_N , which is converted to the duty ratio D by:

$$D(k) = D(k-1) + G_D \times \Delta D_N(k) \quad (8)$$

where G_D is the output scaling factor of the controller.

4. PARTICLE SWARM OPTIMIZATION

4.1. Overview of the PSO Algorithm

The PSO algorithm is based on the collaboration between particles, proposed by R. Eberhart and J. Kennedy in 1995[14] have attracted considerable attention. PSO also is a new branch of population-based heuristic algorithms. The particle swarm is experiencing a growing interest due to simple algorithmic structure and of the fast convergence rate that may be controlled via few parameters.

PSO algorithm can be summarized in the following steps:

1. Initialize each particle vectors of the swarm by assigning a random velocity and position in the problem search space.
2. Compare the particle fitness value with each $pbest$. If the current solution is better than its $pbest$, then update its $pbest$ by the current solution.
3. Finding the best individual $pbest$ in a local search, the competition is one to one, while in the global search, It is necessary to find for the best individual among the swarm as the $gbest$.
4. Updating the velocities using the Eq. 11 and the positions of each particle in the swarm using the Eq. 13.
5. Repeat Steps 2-4 until the stopping criterion is met.

In PSO, each potential solution is represented as a particle. A position x_i and a velocity v_i are associated with each particle. The position and velocity of the i th particle are depicted by

$$x_i = (x_{i,1}, x_{i,2}, \dots, x_{i,N}) \quad (9)$$

$$v_i = (v_{i,1}, v_{i,2}, \dots, v_{i,N}) \quad (10)$$

The position and velocity of each particle are updated according to individual best, $pbest_i^k$, and global best, $gbest_i^k$, using the equations (11) and (13) [12].

The velocity of the particles is depicted in Eq (11)

$$v_i^{k+1} = wV_i^k + c_1r_1(pbest_i^k - x_i^k) + c_2r_2(gbest_i^k - x_i^k) \tag{11}$$

where, V_i^k : current particle velocity, V_i^{k+1} : particle velocity update, $pbest_i^k$: the best position found by the particle, $gbest_i^k$: the best solution found by the swarm.

where c_1 : influence of individual learning rate, c_2 : influence of social learning rate, r_1 and r_2 : two uniformly distributed random in range [0, 1]. w , named the inertia weight, decrease linearly during a run is as given in (12)

$$w = \frac{Iter_{max} - iter}{Iter_{max}} \tag{12}$$

where, $Iter_{max}$ is the maximum number of iteration cycles and $iter$ is the current iteration number.

The position of the particle is shown in Eq (13).

$$X_i^{k+1} = X_i^k + V_i^{k+1} \tag{13}$$

where, X_i^{k+1} is the current particle position, X_i^k is the particle position update.

4.2. Evaluation of the Particle Fitness

The evaluation function for each particle is based on the minimization of integral of error quadratic (IEQ) criterion given by:

$$IEQ = \int_0^{t_f} (P_{max}(t) - P_{PV}(t))^2 dt \tag{14}$$

Where, P_{max} is the maximum power that the panel may issue under the test conditions, P_{PV} is the instant power provided by the PV panel and t_f is the simulation time.

Figure 4 shows the Matlab–Simulink model used to evaluate fitness.

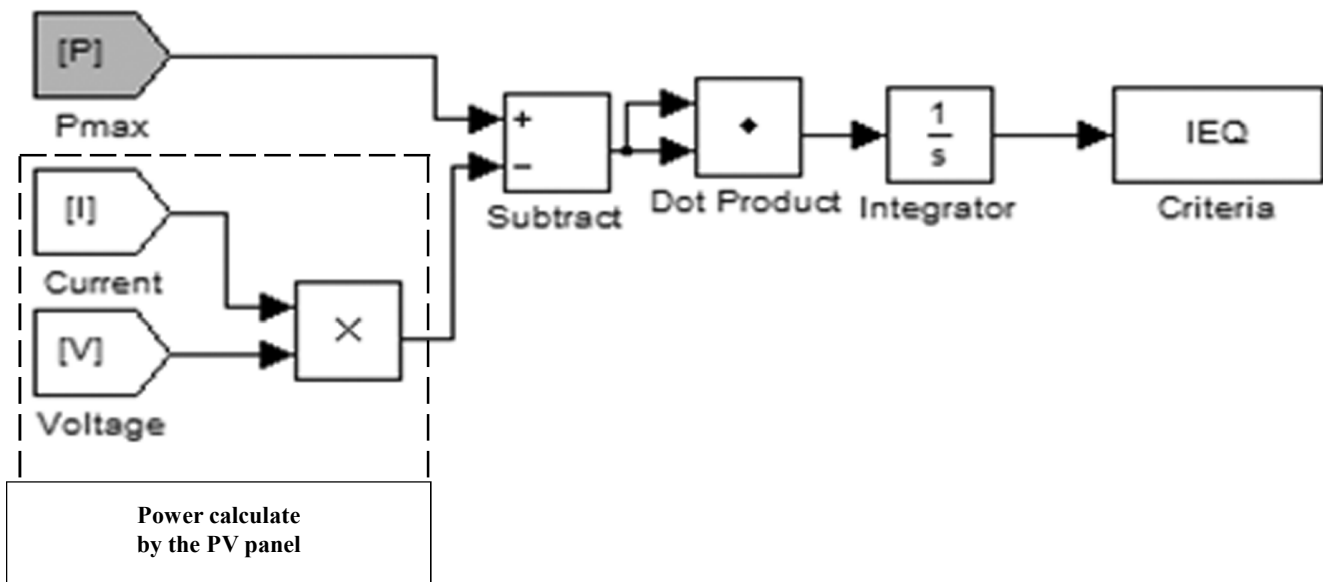


Figure 4: Fitness evaluation with Matlab–Simulink model

5. CONTROL RESULTS

In order to test the robustness of the designed fuzzy controller based MPP tracker under constant and varying atmospheric conditions, various parts of the stand-alone PV system (see Figure 2) using the Matlab/simulink environment. The simulation results are given at a sampling frequency of 100Hz. The setting of membership functions of the controller's variables is depicted as follows:

-In the design of FLC, two inputs variables (e and Δe) and the output variable ΔD characterized by five membership functions are defined respectively on the ranges of variation for input and output $[-35, 5]$, $[-49, 49]$ and $[-3, 3]$. We note here that these intervals were obtained by calculating the maximum and the minimum values allowed for each used variable in our simulated environment for a stand-alone PV system.

Table 2 shows the used electrical data in our MATLAB simulations for a BP SX150S panel manufactured by BP solar company. The best chosen parameters for the PSO algorithm is summarized in Table 3.

Table 2
Parameters of BP SX 150S panel.

<i>Electrical characteristics</i>	<i>Values</i>
No. of modules in series (N_s)	72
No. of modules in series (N_p)	1
Maximum power (P_{max})	150 W
Voltage at P_{max} (V_{max})	34.5 V
Current at P_{max} (I_{max})	4.35 A
Short circuit voltage (I_{sc})	4.75 A
Open circuit voltage (V_{oc})	43.5 V

Table 3
Parameters of PSO used

<i>Parameters</i>	<i>Values</i>
Number of parameters	15
Population size	40
Generations	200
$C_1 = C_2$	2.10

5.1. Stable environmental conditions

Figure 5 shows the evolution of best solutions for 200 generations obtained when PSO algorithm is employed for stand-alone PV system and the convergence towards the minimum error fitness value in few iteration.

Simulation results under two atmospheric conditions, solar irradiance $1000\text{W}/\text{m}^2$ and ambient temperature 25°C , are presented in Figures 6 and 7. We can compare the FLC optimized by PSO and the standard FLC. The duty ratio of the DC-DC boost converter is optimally adjusted as is depicted in Figure 6. It can be seen that the optimized FLC (0.18 s) outperform widely the standard FLC (0.25 s) in response time. Furthermore, the output power of PV panel generated by the optimized FLC is toward of MPP (150 W), while that obtained result by the standard FLC there exceeded largely, shown in Figure 7.

5.2. Simulation under varying atmospheric conditions

Although the ambient temperature during a day doesn't change quickly, a rapid changing temperature is used here to evaluate the effectiveness of the fuzzy controller based MPPT. Simulation results are given in

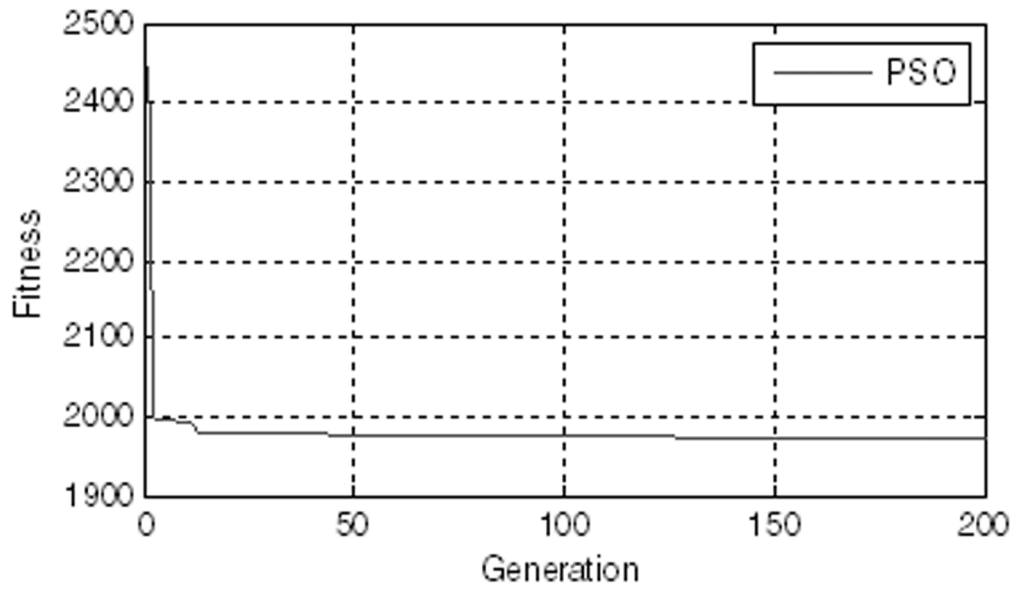


Figure 5: Convergence profile of PSO algorithm for 200 generations.

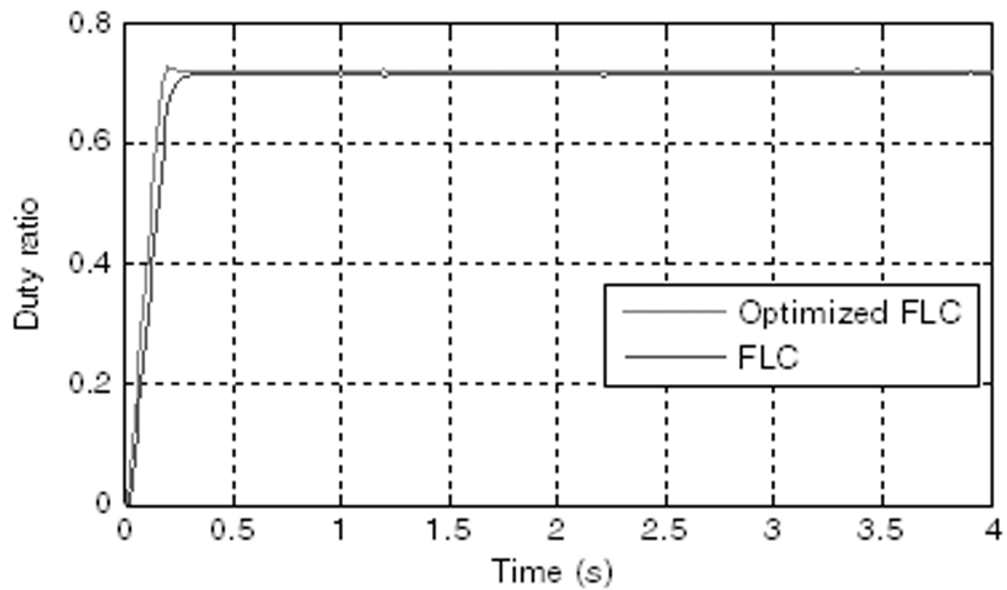


Figure 6: Duty ratio signal under stable environmental conditions.

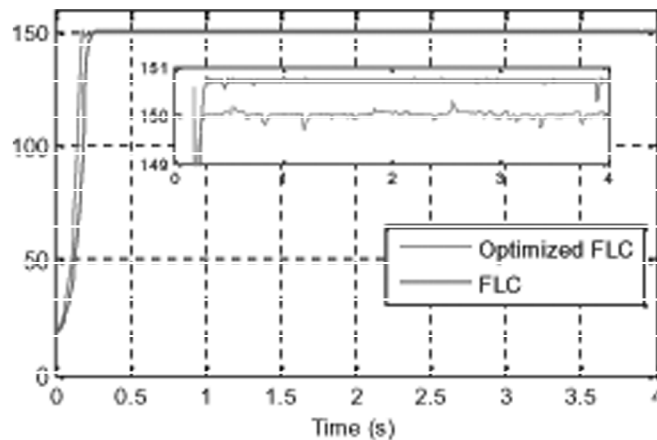


Figure 7: PV panel power under stable environmental conditions.

Figures 10 and 11 under solar radiation $1000\text{W}/\text{m}^2$, a rapid decrease in ambient temperature from 50°C to 25°C over a time period of 2 s, a rapid increase from 25°C to 40°C during 2 s and a slow decrease from 40°C to 35°C over a time period of 7s (see Figure 8).

It can be noted in Figure 9 that the PSO algorithm converges faster to minimum fitness value for 200 generations. The duty ratio of the boost converter is represented in Figure 10. From Figure 11, it can be

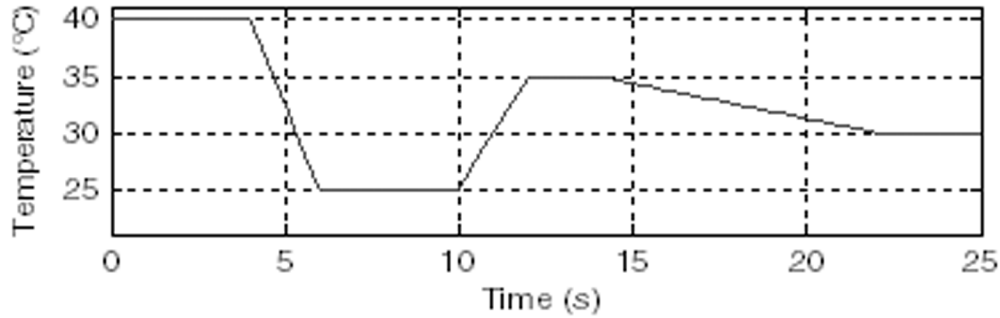


Figure 8: Temperature profile.

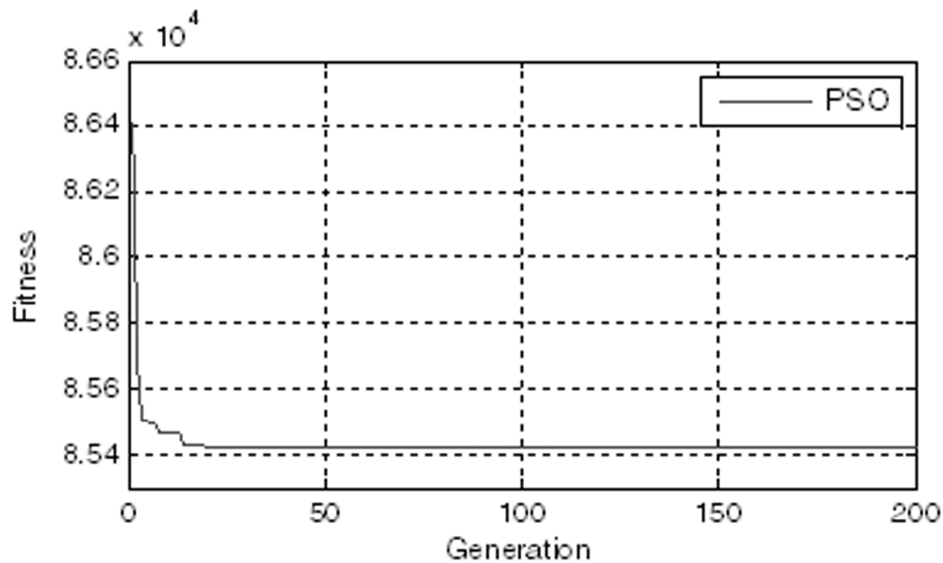


Figure 9: Convergence profile of PSO algorithm for 200 generations.

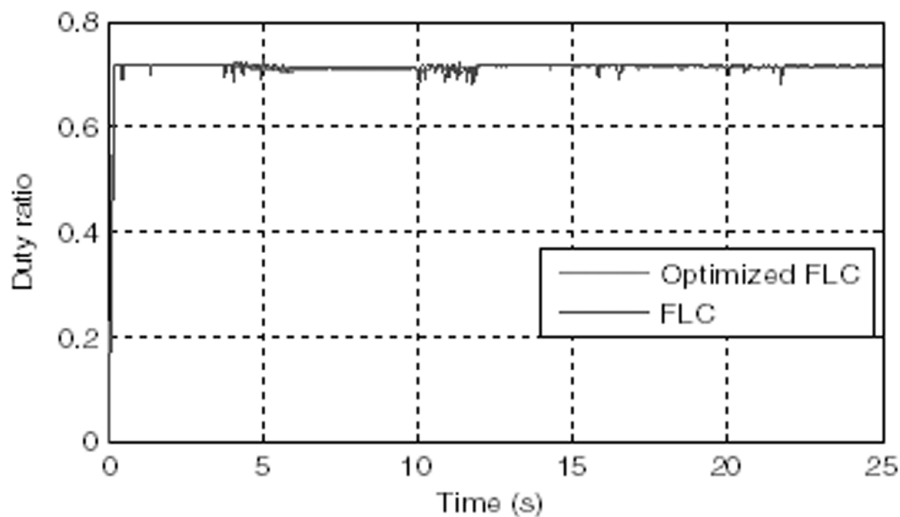


Figure 10: Duty ratio signal under ambient temperature variations.

seen than the optimized FLC reaches the MPP quicker than the standard FLC to reach the same target and also the optimized FLC reduced considerably the oscillations during temperature variations, what the fuzzy controller optimized by PSO more effective and more robust to ambient temperature variations.

In this Figure 12, the ambient temperature is constant 25°C and under solar radiation variations, a rapid increase from $400\text{W}/\text{m}^2$ to $800\text{W}/\text{m}^2$ during 2 s, a rapid increase from $800\text{W}/\text{m}^2$ to $1080\text{W}/\text{m}^2$ during 5 s and a slow decrease from $1080\text{W}/\text{m}^2$ to $800\text{W}/\text{m}^2$ over a time period of 2 s.

As seen from Figure 13, the error fitness profile of the PSO algorithm for 200 generations. Simulation results are shown in Figure 14 and 15. It can be observed that, the optimized FLC is the most efficient and converges quickly to the MPP and with insignificant oscillations. Results show a good robustness of the optimized FLC with respect to irradiance variations.

6. CONCLUSIONS

In this work, a fuzzy controller is used to track the maximum power point in stand-alone PV system. The use of particle swarm optimization to FLCs design holds a great of promise in overcoming two of the major problems in fuzzy controllers design; design time and design optimization. To improve the design and

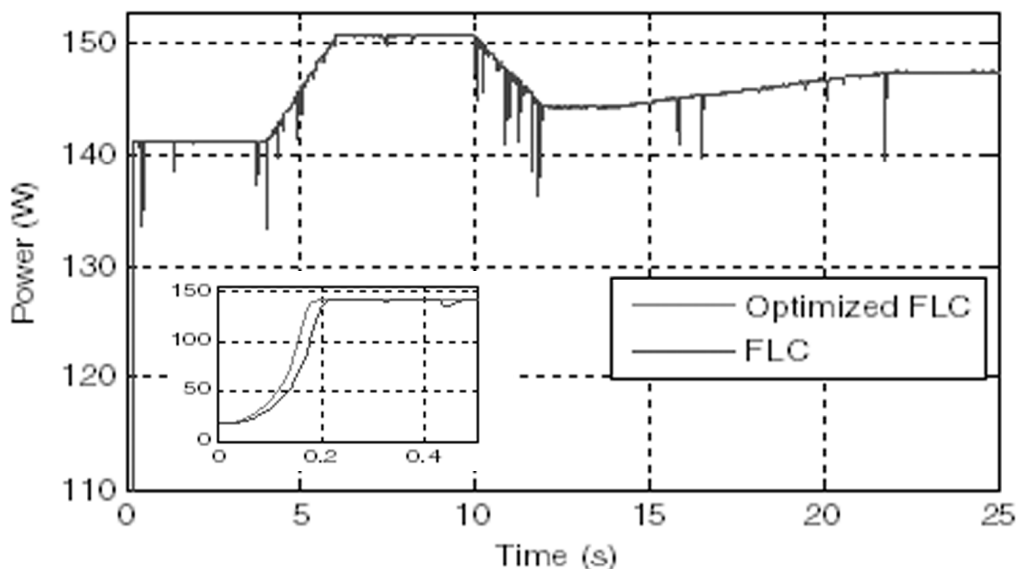


Figure 11: PV panel power under ambient temperature variations.

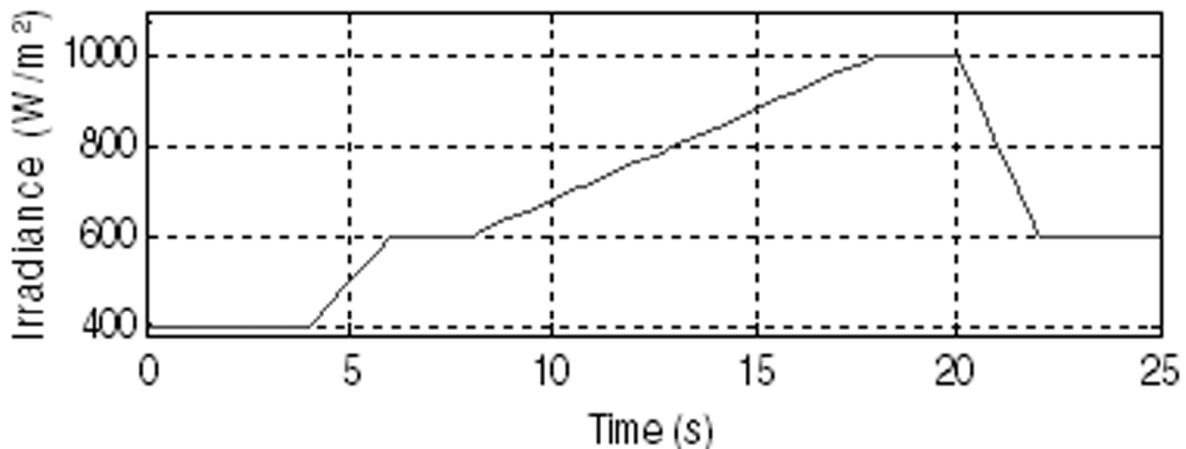


Figure 12: Irradiance profile

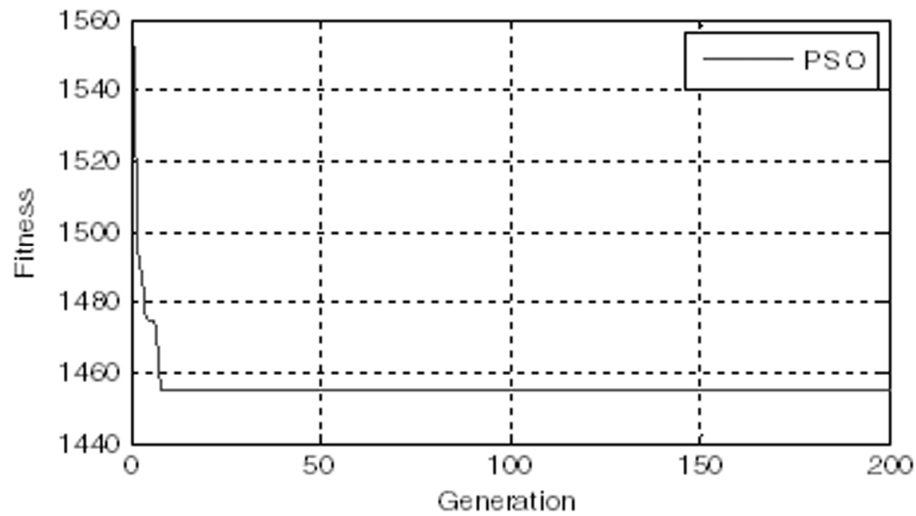


Figure 13: Convergence profile of PSO algorithm for 200 generations

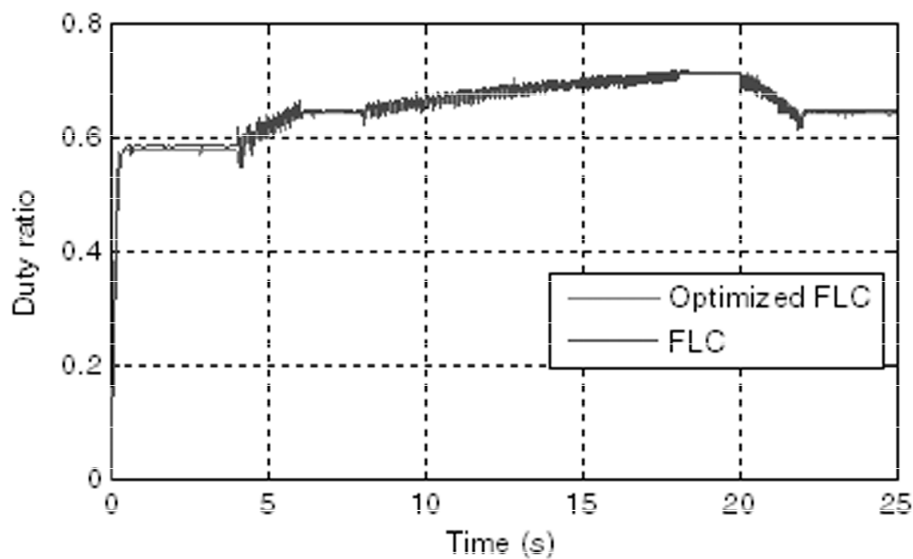


Figure 14: Duty ratio signal under solar radiation variations

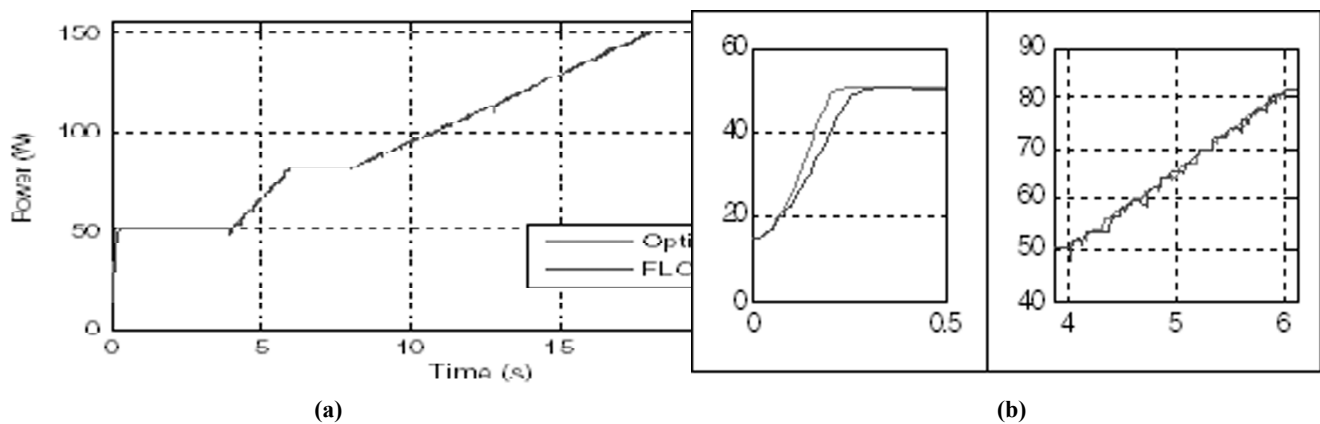


Figure 15: (a) PV panel power under solar radiation variations, (b): Zoom of few sample

further improve the performances of the FLC based MPPT we optimize the membership functions of both input and output controller variables. According to the simulated, the standard FLC design shows much better performances and robustness that of standard FLC under constant and varying atmospheric conditions.

REFERENCES

- [1] R. Vincheh, A. Kargar and G.A. Markadeh, "A hybrid control method for maximum power point tracking (MPPT) in photovoltaic systems," *Arabian Journal for Science and Engineering*, **39** (6), 4715-4725, 2014.
- [2] A. Garrigos, J.L. Lizan, J.M. Blanes and R. Gutierrez, "Combined maximum power point tracking and output current control for a photovoltaic-electrolyser DC/DC converter," *International Journal of Hydrogen Energy*, **39** (36), 20907-20919, 2014.
- [3] V. Salas, E. Olias, A. Barrado and A. Lázaro, "Review of the maximum power point tracking algorithms for stand-alone photovoltaic systems," *Solar Energy Materials and Solar Cells*, **90** (11), 1555-1578, 2006.
- [4] S. Jain and V. Agarwal, "Comparison of the performance of maximum power point tracking schemes applied to single-stage grid-connected photovoltaic systems," *IET Electric Power Applications*, **1** (5), 753-762, 2007.
- [5] J.W. Kimball and P.T. Krein, "Digital ripple correlation control for photovoltaic applications," *Proc. IEEE Annual Power Electronics Specialists Conference*, **PESC-2007**, 1690-1694, 2007.
- [6] W. Xiao and W.G. Dunford, "A modified adaptive hill climbing MPPT method for photovoltaic power systems," *Proc. IEEE Annual Power Electronics Specialists Conference*, Aachen, Germany, **PESC-2004**, 1957-1963, 2004.
- [7] G. Dileep and S.N. Singh, "Maximum power point tracking of solar photovoltaic system using modified perturbation and observation method," *Renewable and Sustainable Energy Reviews*, **50**, 109-129, 2015.
- [8] F. Liu, S. Duan, F. Liu, B. Liu, Y. Kang, "A variable step size INC MPPT method for PV systems," *IEEE Transactions on Industrial Electronics*, **55** (7), 2622-2628, 2008.
- [9] O. Guenounou, B. Dahhou, F. Chabour, "Adaptive fuzzy controller based MPPT for photovoltaic systems," *Energy Conversion and Management*, **78**, 843-850, 2014.
- [10] R. Ramaprabha, M. Balaji, B.L. Mathur, "Maximum power point tracking of partially shaded solar PV system using modified Fibonacci search method with fuzzy controller," *Electrical Power and Energy Systems*, **43**, 754-765, 2012.
- [11] D. Karthik, K. Vijayarekha and S. Raga Subha, "Classifying the suitability of river Cauvery water for drinking using data mining classifiers and authenticating using fuzzy logic," *International Journal of ChemTech Research*, **7** (5), 2203-2207, 2015.
- [12] S. Vaidyanathan, "Adaptive control of Rikitake two-disk dynamo system," *International Journal of ChemTech Research*, **8** (8), 121-133, 2015.
- [13] S. Vaidyanathan, "Adaptive control of the FitzHugh-Nagumo chaotic neuron model," *International Journal of ChemTech Research*, **8** (6), 117-127, 2015.
- [14] S. Vaidyanathan, "Anti-synchronization of Brusselator chemical reaction systems via adaptive control," *International Journal of ChemTech Research*, **8** (6), 759-768, 2015.
- [15] S. Vaidyanathan, "Dynamics and control of Tokamak system with symmetric and magnetically confined plasma," *International Journal of ChemTech Research*, **8** (6), 795-803, 2015.
- [16] D. Karthik and K. Vijayarekha, "Simple and quick classification of soil for sunflower cultivation using data mining algorithm," *International Journal of ChemTech Research*, **7** (6), 2601-2605, 2015.
- [17] N. Khaehintung and P. Sirisuk, "Implementation of maximum power point tracking using fuzzy logic controller for solar-powered light-flasher applications," *Proc. 47th IEEE International Midwest Symposium on Circuits and Systems*, Hiroshima, **MWSCAS-2004**, 171-174, 2004.
- [18] A. Khare and S. Rangnekar, "A review of particle swarm optimization and its applications in solar photovoltaic system," *Applied Soft Computing*, **13**, 2997-3006, 2013.
- [19] R. Eberhart, "A new optimizer using particle swarm theory," *Proc. Sixth International Symposium on Micro Machine and Human Science*, **MHS-1995**, 39-44, 1995.
- [20] S. Monisa and S. Vijayachitra, "Real time performance analysis and fault diagnosis in heat exchanger," *International Journal of ChemTech Research*, **8** (12), 418-427, 2015.
- [21] A. Bouguerne, A. Lebaroud and A. Boukadoum, "Clustering optimized analytic vibration signal of rolling bearing faults using K-means algorithm," *International Journal of ChemTech Research*, **9** (4), 400-406, 2016.
- [22] J. Kennedy and R. Eberhart, "Particle swarm optimization," *Proc. IEEE International Conference on Neural Networks*, Perth, Western Australia, **ICNN-1995**, 1942-1947, 1995.
- [23] A. Prathik, K. Uma and J. Anuradha, "An overview of application of graph theory," *International Journal of ChemTech Research*, **9** (2), 242-248, 2016.
- [24] J. Brownlee, *Clever Algorithms: Nature-Inspired Programming Recipes*, LuLu, 2012.

- [25] S. Vaidyanathan, "A novel 3-D conservative chaotic system with sinusoidal nonlinearity and its adaptive control", *International Journal of Control Theory and Applications*, **9** (1), 115-132, 2016.
- [26] S. Vaidyanathan and S. Pakiriswamy, "A five-term 3-D novel conservative chaotic system and its generalized projective synchronization via adaptive control method", *International Journal of Control Theory and Applications*, **9** (1), 61-78, 2016.
- [27] S. Vaidyanathan, K. Madhavan and B.A. Idowu, "Backstepping control design for the adaptive stabilization and synchronization of the Pandey jerk chaotic system with unknown parameters", *International Journal of Control Theory and Applications*, **9** (1), 299-319, 2016.
- [28] A. Sambas, S. Vaidyanathan, M. Mamat, W.S.M. Sanjaya and R.P. Prastio, "Design, analysis of the Genesio-Tesi chaotic system and its electronic experimental implementation", *International Journal of Control Theory and Applications*, **9** (1), 141-149, 2016.
- [29] S. Vaidyanathan and A. Boulkroune, "A novel hyperchaotic system with two quadratic nonlinearities, its analysis and synchronization via integral sliding mode control," *International Journal of Control Theory and Applications*, **9** (1), 321-337, 2016.
- [30] S. Sampath, S. Vaidyanathan and V.T. Pham, "A novel 4-D hyperchaotic system with three quadratic nonlinearities, its adaptive control and circuit simulation," *International Journal of Control Theory and Applications*, **9** (1), 339-356, 2016.
- [31] Z. Ahmad and S.N. Singh, "Extraction of the internal parameters of solar photovoltaic module by developing Matlab / Simulink based model," *International Journal of Applied Engineering Research*, **7** (11), 1-5, 2012.
- [32] K.Kanimozhi and B. Raja Mohamed Rabi, "Parameter analysis method for enhancing efficiency of photovoltaic cells," *International Journal of ChemTech Research*, **9** (1), 276-281, 2016.
- [33] N. Mohan, T.M. Undeland and W.P. Robbins, *Power Electronics – Converters, Applications, and Design*, 2nd edition, Wiley, 1995.
- [34] T. Florence, S.Dharmalingam, V. Ragupathy and P. Satishkumar, "Machinability study on electrochemical machining – a review", *International Journal of ChemTech Research*, **7** (6), 2596-2600, 2015.
- [35] S. Lekhchine, T. Bahi, I. Abadlia and H. Bouzeria, "Neuro-speed controller of five phase induction motor driven using direct torque control strategy," *International Journal of ChemTech Research*, **9** (4), 555-565, 2016.